2015 (1962).
[22]V. M. Ellsworth and J. J. Hopfield, Phys. Rev. 29, 79 (1927).
[23]R. S. Mulliken, and D. S. Stevens, Phys. Rev. 44, 720 (1933).
[24]R. W. Nicholls, Can. J. Phys. 43, 1390 (1965).
[25]R. C. Evans, *Crystal Chemistry* (Cambridge U. P., Cambridge, England, 1966), pp. 74 and 112.

PHYSICAL REVIEW B VOLUME 6, NUMBER 8 15 OCTOBER 1972

Oblique Polaritons in Uniaxial Crystals: Application to $LiIO_3$ †

W. S. Otaguro, E. Wiener-Avnear,* S. P. S. Porto, and J. Smit
Departments of Physics and Electrical Engineering, University of Southern California, Los Angeles, California 90007
(Received 28 January 1972)

In Raman scattering involving polaritons propagating at arbitrary oblique angles with respect to the crystallographic axes, the selection rules derived for polaritons propagating along the crystal axes are no longer obeyed. We present the analysis of oblique polaritons which account for their frequency dispersion as a function of both the magnitude and the direction of the wave vector $\vec{k}$. Application of this theory to the experimental results obtained for $LiIO_3$ easily clarifies the appearance of "new" lines in the polariton region.

INTRODUCTION

Raman scattering for phonons propagating along the crystallographic axes is well understood in terms of the selection rules provided by group theory.[1] Also, the dispersion in the polariton region associated with the variation of the magnitude of the wave vector $\vec{k}$ of the phonon, again directed along the crystallographic axes, has been shown to agree with theory.[2-5] However, when the phonon is not propagating along the crystallographic axis (oblique phonon), "new" frequencies occur which seem to violate the selection rules.

The occurrence of this angular dispersion was first noted by Poulet,[6] by Ketelaar *et al.*,[7] and by Couture-Mathieu *et al.*[8] An approximate theory for the angular dispersion in crystals with two atoms per unit cell was given by Loudon.[9] This theory was used for the Raman effect by Damen *et al.*[10] in the study of the Raman spectra of ZnO. Arguello *et al.*[11] provided an extensive discussion of Loudon's model in their analysis of the first-order Raman effect in wurtzite-type crystals. These early works merely analyzed the Raman spectra where the phonons outside of the polariton region were propagating midway between two crystallographic axes. An attempt was made to study the experimental results of angular dispersion in $LiIO_3$ for 90° Raman scattering.[12] Although the agreement between the theory and the experimental results was fair, $LiIO_3$, being a uniaxial crystal with C_6^6 symmetry and two molecules per unit cell, presented a more complicated problem than that of the wurzite crystals upon which Loudon's derivations were based.[9] It was evident that a more general expression for the angular dispersion was needed.

In studying $NaNO_2$ Hartwig *et al.*[13] used the electrostatic approximation to explain the angular dispersion of the oblique phonons outside the polariton region ($k^2c^2/\omega^2 > \epsilon_0$). For oblique phonons propagating in a major crystallographic plane, frequency gaps occur. The frequency gaps are determined by the transverse optic (TO) and longitudinal optic (LO) end-point frequencies, which characterize the phonons propagating along the crystallographic axes with monotonically varying angular dispersion curves. Using Eq. (3) of Ref. 13 for the angular dispersion in $LiIO_3$ studied earlier,[12] the agreement between experiment and theory was excellent.[14] Thus the angular dispersion outside the polariton region is quite well explained. However, in the polariton region, the electrostatic approximation is no longer valid.[13] The derivation of the angular dispersion must now include the magnetic fields.

We report the theoretical and experimental re-

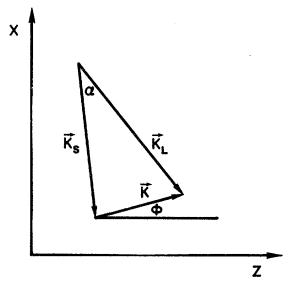

FIG. 1. Conservation of momentum. The forward-scattering angle is represented by α. The angle between the propagation direction of the polariton and the z axis is represented by ϕ.

sults of the angular dispersion of oblique polaritons in $LiIO_3$ for several forward Raman-scattering angles.

THEORY

Retaining the time derivatives of all the electromagnetic fields propagating in an insulator and assuming the time variations of the fields proportional to $e^{-i\omega t}$, Maxwell's equations give

$$\nabla(\nabla\cdot\vec{E}) - \nabla^2\vec{E} = (\omega^2/c^2)\overleftrightarrow{\epsilon}\cdot\vec{E}, \tag{1}$$

where $\overleftrightarrow{\epsilon}$ is the dielectric constant tensor and μ is equal to unity. The operation indicated by the ∇ operator can be replaced by $(i\vec{k})$ and Eq. (1) becomes

$$\vec{k}(\vec{k}\cdot\vec{E}) - k^2\vec{E} = -(\omega^2/c^2)\overleftrightarrow{\epsilon}\cdot\vec{E}\ . \tag{2}$$

Dividing by k^2 and defining the propagation vector

$$\vec{s} = \vec{k}/k = \alpha_1\hat{i} + \alpha_2\hat{j} + \alpha_3\hat{k},$$

Eq. (2) becomes

$$\vec{s}(\vec{s}\cdot\vec{E}) - (1 - \overleftrightarrow{\epsilon}/n^2)\cdot\vec{E} = 0\ , \tag{3}$$

where α_i are the direction cosines of the wave vector $\vec{k}$ with respect to the principal axes of the dielectric constant tensor $\overleftrightarrow{\epsilon}$;

$$n^2 = c^2k^2/\omega^2. \tag{4}$$

When the principal crystallographic axes of the crystal $\vec{k}$ with respect to the principal axes of Eq. (3),

$$\begin{vmatrix} \alpha_1^2 - (1 - \epsilon_1/n^2) & \alpha_2\alpha_1 & \alpha_3\alpha_1 \\ \alpha_1\alpha_2 & \alpha_2^2 - (1 - \epsilon_2/n^2) & \alpha_3\alpha_2 \\ \alpha_1\alpha_3 & \alpha_2\alpha_3 & \alpha_3^2 - (1 - \epsilon_3/n^2) \end{vmatrix} = 0\ , \tag{5}$$

can be reduced to

$$\alpha_1^2\left(\frac{1}{n^2} - \frac{1}{\epsilon_2}\right)\left(\frac{1}{n^2} - \frac{1}{\epsilon_3}\right) + \alpha_2^2\left(\frac{1}{n^2} - \frac{1}{\epsilon_1}\right)\left(\frac{1}{n^2} - \frac{1}{\epsilon_3}\right) + \alpha_3^2\left(\frac{1}{n^2} - \frac{1}{\epsilon_1}\right)\left(\frac{1}{n^2} - \frac{1}{\epsilon_2}\right) = 0. \tag{6}$$

This is essentially Fresnel's equation[15] in which form it has been presented by Borstel and Merten,[16] who derived it using lattice dynamics in conjunction with Maxwell's equations. The form of Eq. (6) allows it to be applied for propagation along principal crystallographic axes or in planes.

The dielectric constant is not a constant of the material but may depend on frequency and wavelength. However, in the long-wavelength limit where Raman experiments are conducted, the dielectric constant is only a function of frequency ω. In crystals of low symmetry, this could imply that the orientation of the principal axes of the dielectric tensor depends on ω. For crystals with at least two twofold axes or one threefold axis (cubic, orthorhombic, uniaxial) the $\overleftrightarrow{\epsilon}$ tensor is diagonal with respect to the crystallographic axes. We will therefore restrict our analysis to these crystals. Also we will only consider angular dispersion in a plane of inequivalent crystallographic axes. Therefore Eq. (6) will have the following solutions ($\alpha_3 = 0$):

$$\frac{1}{n^2} - \frac{1}{\epsilon_3} = 0, \tag{7}$$

$$\alpha_1^2\left(\frac{1}{n^2} - \frac{1}{\epsilon_2}\right) + \alpha_2^2\left(\frac{1}{n^2} - \frac{1}{\epsilon_1}\right) = 0. \tag{8}$$

Equation (7) represents the solution for the ordinary wave and Eq. (8) represents the solution for the extraordinary wave which exhibits the angular dispersion.

Generally, the characteristic features of the examined crystal are contained in the dielectric constants $\epsilon_i(\omega)$ in Eq. (8), which are determined by the TO and LO frequencies of the optical phonons along the principal axes

$$\epsilon_i(\nu_\phi) = \epsilon_i^\infty \prod_{j=1}^{N_i} \frac{(\nu_{ij}^{LO})^2 - \nu_\phi^2}{(\nu_{ij})^2 - \nu_\phi^2}\ , \tag{9}$$

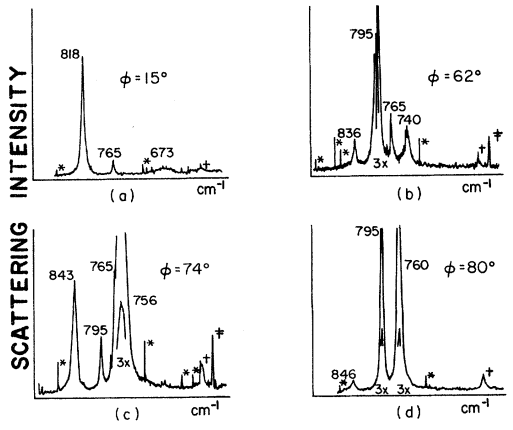

FIG. 2. Typical angular dispersion spectra of oblique polaritons in $LiIO_3$ for $\alpha = 1.4°$. The frequency is given in wave numbers. The asterisks represent the wave-number calibration marks. The dagger marks a benzene line. The double dagger marks an argon fluorescence.

tensor, and ϵ_0 is the permittivity where i represents the x, y, or z principal axes; ν_ϕ is the frequency of the oblique polariton; ν_{ij}, ν_{ij}^{LO} are the TO and LO frequencies, respectively, of the symmetry mode polarized along the ith axis; and N_i is the total number of modes j polarized along the ith direction. Inserting Eq. (9) into Eq. (8) gives

$$\tan^2\phi = -\left(\frac{1}{n^2} - \frac{1}{\epsilon_2^\infty}\prod_{i=1}^{N_2}\frac{(\nu_{2i})^2-\nu_\phi^2}{(\nu_{2i}^{LO})^2-\nu_\phi^2}\right)\Big/ \left(\frac{1}{n^2} - \frac{1}{\epsilon_1^\infty}\prod_{j=1}^{N_1}\frac{(\nu_{1j})^2-\nu_\phi^2}{(\nu_{1j}^{LO})^2-\nu_\phi^2}\right), \quad (10)$$

where ϕ is the angle between the oblique-polariton propagation direction and crystallographic axis 1 (Fig. 1) and ϵ_i^∞ is the high-frequency dielectric constant along the ith crystallographic axis. The damping has been ignored in this discussion.

Outside the polariton region, namely, $n^2 = k^2c^2/\omega^2 \gg \epsilon_0$, but where $\vec{k}$ is still near the center of the Brillouin zone, $(1/n^2)$ in Eq. (10) can be neglected (reducing it to the electrostatic approximation); this was done by Hartwig *et al.*[13]

The momentum transfer $\vec{k}$ in Fig. 1 can be obtained from the law of cosines; $k^2 = k_L^2 + k_S^2 - 2k_Lk_S\cos\alpha$, where k_L, k_S are the wave vectors of the incident laser and scattered light, respectively, and α is the angle between k_L and k_S. With wave vectors related to the index of refraction by $k_i^2 = (2\pi n_i\nu_\phi/c)^2$, Eq. (10) becomes

$$\tan^2\phi = -\left(\frac{\nu_\phi^2}{n_L^2\nu_L^2 + n_S^2\nu_S^2 - 2n_Ln_S\nu_L\nu_S\cos\alpha} - \frac{1}{\epsilon_X^\infty}\prod_{j=1}^{N_X}\frac{(\nu_{E_1j})^2-\nu_\phi^2}{(\nu_{E_1j}^{LO})^2-\nu_\phi^2}\right)\Big/ \left(\frac{\nu_\phi^2}{n_L^2\nu_L^2 + n_S^2\nu_S^2 - 2n_Ln_S\nu_L\nu_S\cos\alpha} - \frac{1}{\epsilon_Z^\infty}\prod_{i=1}^{N_Z}\frac{(\nu_{Ai})^2-\nu_\phi^2}{(\nu_{Ai}^{LO})^2-\nu_\phi^2}\right), \quad (11)$$

where n_L and n_S are the index of refraction of the incident laser and scattered light, respectively, ν_L is the frequency of the laser, and $\nu_S = \nu_L - \nu_\phi$ is the Stokes frequency. In the experimental arrangement used, $(\gamma x + \beta z)(yy)(\beta x - \gamma z)$, where $\gamma^2 + \beta^2 = 1$, n_L and n_S are equal to n_{E_1}.

EXPERIMENT AND RESULTS

Forward-scattering geometry is used to obtain the oblique polaritons (Fig. 1). The amount of scattered spurious light is reduced by an iodine filter.[17] The problem of multiple internal reflections within the crystal, which produce additional lines in the spectra, was minimized by index matching. The polished single crystal of $LiIO_3$ was immersed in a cell of benzene. The oblique polaritons are propagated in the xz plane by simply rotating the crystal around its y axis. The extraordinary (yy) Raman polarization filter was used.

The experiment observed the oblique polariton of the upper two branches in $LiIO_3$ at $\alpha \approx 1°$. Some typical spectra are shown in Fig. 2. The experimental results are shown in Fig. 3. The two sets of experimental runs were best fitted [Eq. (11)] with the scattering angles $\alpha = 0.9°$ and $\alpha = 1.4°$. For comparison, the oblique phonon for $\alpha = 90°$ is also shown in Fig. 3.[14] The oblique phonons in the LO region were used to determine the propagation angle ϕ of the corresponding oblique polaritons in the TO region. The oblique phonons in the LO region show considerably less variation than in the TO region as α is varied, since for the LO oblique

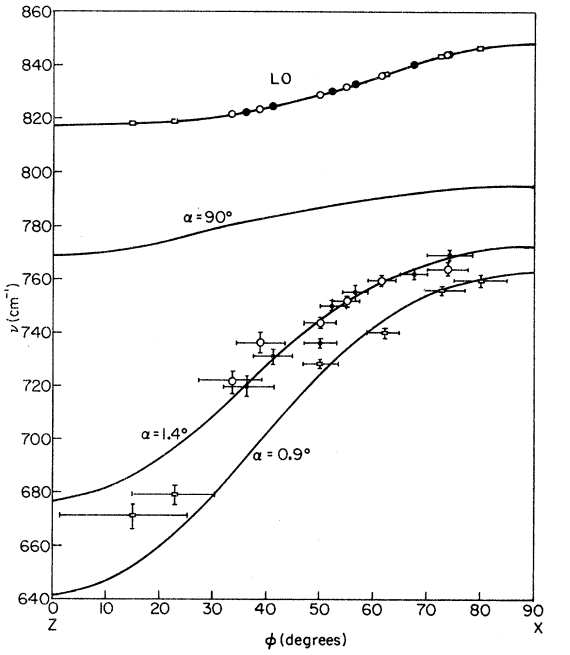

FIG. 3. Comparison of experimental data with Eq. (11) for $\alpha = 1.4°$ and $\alpha = 0.9°$. The open and closed circles represent spectra taken at $\alpha = 1.4°$. The open squares represent spectra taken at $\alpha = 0.9°$. The experimental oblique-polariton points were positioned using the LO curve. The $\alpha = 90°$ oblique phonon curve represents the correct angular dispersion for the $E_{1\,TO}$(769 cm^{-1}) to A_{TO}(795 cm^{-1}). The results published earlier (Ref. 12) were miscalibrated by approximately 9 cm^{-1}.

phonon, $[n(\nu_\phi)]^2 > \epsilon(\nu_\phi)$. This method provides a systematic means for determining the angle ϕ. The horizontal lines through the polariton data points represent the estimated error in the determination of the oblique angle ϕ through this method. The vertical bars through the data points represent the error due to the linewidth of the observed peaks. The experiment agrees quite well with theory.

DISCUSSION

The curves for the A and E_1 extraordinary polariton modes of $LiIO_3$ are plotted in Fig. 4 using the values for the LO and TO frequencies as reported in Ref. 14. The solid line represents the A symmetry polaritons and the dotted curves represents the E_1 symmetry polaritons. The LO modes observed in the polariton region exhibit no frequency dispersion as the magnitude of $\vec{k}$ is changed; however, these modes will exhibit an angular dispersion when the direction of their $\vec{k}$ is at some oblique angle with respect to the crystallographic axes. The cross-hatched area represents the regions where the oblique polaritons may occur as the direction of $\vec{k}$ is varied. Thus, while the magnitude of $\vec{k}$ is held almost constant, the oblique polaritons will vary in frequency according to Eq. (11) as the propagation direction $\vec{s}$ is varied. Previous experiments[11,13] in which $\vec{s}$ is varied required a change in the experimental scattering geometry. However, in $LiIO_3$ the angular dispersion of the oblique extraordinary (yy) polaritons was easily obtained by rotating the crystal around its y axis. Although a large-frequency tuning range was obtained in the oblique-polariton experiments, the cross section of the oblique polaritons being observed will increase or decrease with ϕ, depending on the Raman polarization filter being used.[18] The application of this technique of oblique phonons and polaritons for tuning a stimulated Raman system assures stability and wide range frequency tunability in the infrared region (Fig. 4); however, the drastic change in the scattering efficiency at different angles may limit its usability.

At large scattering angles, $\alpha = 90°$, the scattering cross sections of the oblique phonons were well explained.[18] In the polariton region the scattering cross section is more difficult to determine due

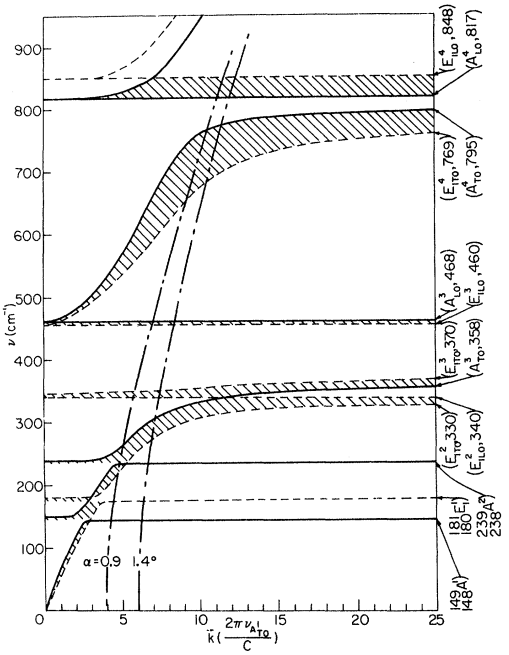

FIG. 4. Polariton curves for the A (solid curves) and E_1 (dotted curves) in $LiIO_3$. The cross-hatched regions represent the areas where oblique polaritons may be observed. The dash-dotted lines represent the equations of conservation of energy and momentum.

to the forward-scattering experimental arrangement. However, an interesting resonance occurs as the oblique-polariton frequency coincides with the 765-cm^{-1} E_2 phonon (see Fig. 2). Efforts are presently under way to study this resonance.

Owing to the large frequency variations of the polaritons when propagating at oblique angles, it is essential in all experiments to verify not only the magnitude but also the propagation direction of the oblique polaritons in order to properly determine the nature of the frequencies observed. The generality of the derivation used allows Eq. (11) to be applied to determine the frequency dispersion of the oblique polaritons at any ω-vs-$|\vec{k}|$ region and for any propagation direction in a major plane of crystals of cubic, uniaxial, or orthorhombic biaxial symmetries.

---

†Work supported by the National Science Foundation.

*Present address: Physics Department, University of Negev, Beer-Sheva, Israel.

[1]S. P. S. Porto, in *Proceedings of the International Conference on Light Scattering Spectra in Solids, New York University*, 1968, edited by G. B. Wright (Springer-Verlag, New York, 1969).

[2]C. V. Henry and J. J. Hopfield, Phys. Rev. Letters 15, 964 (1965).

[3]S. P. S. Porto, B. Tell, and T. C. Damen, Phys. Rev. Letters 16, 450 (1966).

[4]J. F. Scott, L. E. Cheesman, and S. P. S. Porto, Phys. Rev. 162, 834 (1967).

[5]E. Burnstein, S. Ushioda, A. Pinczuk, and J. F. Scott, in Ref. 1.

[6]H. Poulet, Compt. Rend. 234, 2185 (1952); Ann. Phys. (Paris) 10, 908 (1955).

[7]J. A. A. Ketelaar, C. Haas, and J. Fahrenfort,

Physica 20, 1259 (1954).
[8]L. Couture-Mathieu, J. A. A. Ketelaar, W. Vedderand, and J. Fahrenfort, Physica 18, 762 (1952); J. Chem. Phys. 20, 1492 (1952).
[9]R. Loudon, Advan. Phys. 13, 423 (1964).
[10]T. C. Damen, S. P. S. Porto, and B. Tell, Phys. Rev. 142, 570 (1966).
[11]C. A. Arguello, D. L. Rousseau, and S. P. S. Porto, Phys. Rev. 181, 1351 (1969).
[12]W. Otaguro, C. A. Arguello, and S. P. S. Porto, Phys. Rev. B 1, 2818 (1970).
[13]C. M. Hartwig, E. Wiener-Avnear, J. Smit, and S. P. S. Porto, Phys. Rev. B 3, 2078 (1971).
[14]W. S. Otaguro, E. Wiener-Avnear, and S. P. S. Porto, Phys. Rev. B 4, 4542 (1971).
[15]M. Born and E. Wolf, *Principles of Optics* (Pergamon, London, 1965).
[16]G. Borstel and L. Merten, Z. Naturforsch. 26a, 653 (1971).
[17]L. Fraas, thesis (University of Southern California, 1971) (unpublished).
[18]W. S. Otaguro, E. Wiener-Avnear, and S. P. S. Porto, Appl. Phys. Letters 18, 499 (1971).

PHYSICAL REVIEW B VOLUME 6, NUMBER 8 15 OCTOBER 1972

Fundamental Absorption Edge of $SrTiO_3$

David Redfield and William J. Burke
RCA Laboratories, Princeton, New Jersey 08540
(Received 27 January 1972)

Detailed measurements of the fundamental absorption edge of $SrTiO_3$ between 6 and 300 K are reported. Because these results provide the first detailed data below 82 K, several new properties of this material have been observed. The energies of the fundamental transitions are found to have unusually small temperature dependence. It is also observed that the strengths of the phonon-emission and impurity-induced absorption processes are more strongly temperature dependent than is found in other materials. In addition, we propose a different explanation for the prominent shoulder in the absorption at 3.40 eV: that it is merely the saturation of the phonon-assisted transitions.

I. INTRODUCTION

Among the many interesting properties of $SrTiO_3$, optical phenomena such as luminescence[1] and photochromicity[2] have gained much recent interest. It has been found that a full understanding of these phenomena depends upon a knowledge of the fundamental absorption process of the crystal on which we report here. In addition, detailed information on the fundamental optical transitions should aid in the elucidation of the electronic energy band structure of the material, which is not well established.

In $SrTiO_3$ the Kahn-Leyendecker band-structure calculation[3] indicates that the lowest energy gap may be indirect from Γ_{15} to X_3. Baer[4] has concluded from his interband Faraday rotation data, however, that the transition is direct and most probably at the Γ point. DiDomenico and Wemple[5] concluded from their high-temperature results in $BaTiO_3$ that the absorption edge is direct from X_5' to X_3 and the lower-energy phonon-assisted $\Gamma_{15} \rightarrow X_3$ process is masked by the stronger direct transition. They expected that, because of the similarity of $BaTiO_3$ and $SrTiO_3$, these latter conclusions should apply for $SrTiO_3$. Capizzi and Frova[6] concluded from their absorption measurements that the absorption edge is the $\Gamma_{15} \rightarrow X_3$ phonon-assisted process and that the shoulder at 3.40 eV is the direct $X_5' \rightarrow X_3$ transition.

Past experimental data on the fundamental absorption edge of $SrTiO_3$ have been limited. The first transmission measurements[7] of the absorption edge reported exponential spectral shapes whose temperature dependence was claimed to follow Urbach's rule.[8] However, Capizzi and Frova's measurement[6] between 300 and 82 K showed a change from exponential shape at room temperature to a structured edge characteristic of single phonon-assisted transitions.

The present paper reports similar transmission measurements, but carried to much lower temperatures and to higher precision. These features of the experiments have revealed several unexpected properties of the temperature dependence of the absorption edge and confirmed its phonon-assisted nature. These properties are: (i) The threshold energies of the different components of the edge are essentially temperature independent; (ii) the energy at which the absorption saturates (near 5000 cm^{-1}) is similarly insensitive to temperature; (iii) the strengths of the electronic transitions assisted by phonon emission and by impurities are more strongly temperature dependent than in any other known case.